Chirality Transfer in 1D Self-Assemblies

Shchyrba, Aneliia; Manh-Thuong Nguyen, [No Value]; Waeckerlin, Christian; Martens, Susanne; Nowakowska, Sylwia; Ivas, Toni; Roose, Jesse; Nijs, Thomas; Boz, Serpil; Schaer, Michael

Published in:
Journal of the American Chemical Society

DOI:
10.1021/ja407315f

Publication date:
2013

Chirality Transfer in 1D-Self-assemblies: Influence of H-bonding vs. Metal Coordination between Dicyano[7]helicene Enantiomers

Aneliia Shchyrba,[1] Manh-Thuong Nguyen,[2] Christian Wäckerlin,[3] Susanne Martens,[1] Sylwia Nowakowska,[1] Toni Ivas,[1] Jesse Roose,[4] Thomas Nijs,[1] Michael Schär,[4] Meike Stöhr,[5] Carlo A. Pignedoli,[6] Carlo Thilgen,[4] François Diederich,[4] Daniele Passerone,[6] and Thomas A. Jung.[3*]

1. Department of Physics, University of Basel, Klingelbergstrasse 82, 4056 Basel, Switzerland
2. The Abdus Salam International Centre for Theoretical Physics, Strada Costiera 11, I - 34151 Trieste, Italy
3. Laboratory for Micro- and Nanotechnology, Paul Scherrer Institute, 5232 Villigen PSI, Switzerland
4. Laboratorium für Organische Chemie, ETH Zurich, Wolfgang-Pauli-Strasse 10, 8093 Zürich, Switzerland
5. Zernike Institute for Advanced Materials, University of Groningen, Nijenborgh 4, 9747 AG Groningen, The Netherlands
6. Empa, Swiss Federal Laboratories for Materials Science and Technology, Nanotech & Surfaces Laboratory, Überlandstrasse 129, 8600 Dübendorf, Switzerland

Supporting Information Placeholder

ABSTRACT: Chiral recognition as well as chirality transfer in supramolecular self-assembly and on-surface coordination is studied for the enantiopure 6,13-dicyano[7]helicene building block. Remarkable about this helical molecule is that both H-bonded chains and metal-coordinated chains can be formed on the same substrate, thereby allowing for a direct comparison of the chain bonding motifs and their effects on the self-assembly in experiment and theory. Conformational flexure, adsorbate-adsorbent and intermolecular interactions can be identified as factors influencing the chiral recognition at the binding site. The observed H-bonded chains are chiral, however the overall appearance of Cu-coordinated chains is no longer chiral. The study was performed via Scanning Tunneling Microscopy (STM), X-ray-Photoelectron Spectroscopy (XPS), and Density Functional Theory (DFT) calculations. We show a significant influence of the molecular flexibility and the type of bonding motif on the chirality transfer in the 1D self-assembly.

Controlling and understanding chirality in chemical reactions and during self-assembly is important, in particular if chiral or pro-chiral building blocks[1] are involved.[2,3] Recently, a Pasteur type[4] spontaneous chiral resolution has been shown to occur also in two dimensions, at surfaces.[2,5–7] In analogy to the 3D case, the condensation of 2D islands at surfaces can be controlled by the enantiomeric excess[8,9] of one component or by a chiral auxiliary.[10] Chirality transfer and the long-range expression of chirality in molecular self-assembly have been studied intensively in surface science. These studies involved pro-chiral molecules[10,11] which become chiral by conformational changes induced by their interaction with the substrate, as well as inherently chiral molecules. A very interesting model system is provided by [*n*]helicenes, because they have been used to study the transfer of chirality during nucleation and self-assembly at the solid-liquid interface,[12] as well as at the solid-vacuum interface.[13,14] Chiral interactions were observed neither for layers of hexathia[11]helicene on Au(111) nor for linear admolecular chains on Au(110).[15] Parschau et al. studied the chirality transfer of [7]helicene in the growth of 2D islands by van-der-Waals (vdW) interactions.[16] Later, Stöhr et al. showed the spontaneous resolution of (±)-6,13-dicyano[7]helicene driven by polar interactions,[17] and Seibel et al. described the 2D separation of pentahelicene into homochiral domains purely through vdW forces.[18] Notably, only a few investigations on chiral molecules self-assembling to structures of further reduced dimensionality, i.e. 1D, have been reported: On calcite, Kühnle and coworkers observed islands of enantiopure [7]helicene-2-carboxylic acid and chains of the racemate, both stabilized by π-π stacking.[19–21] The present article reports on the chirality transfer which takes place during the self-assembly of enantiopure dicyanohelicene building blocks into 1D chains, a particular focus being put on the influence of the intermolecular bonding motif.

With enantiomers of cyano-functionalized helicenes, (*P*)-(+)-6,13-dicyano[7]helicene and (*M*)-(–)-6,13-dicyano[7]helicene ((*P*)-**1** and (*M*)-**1**) (Fig. 1), we earlier introduced an inherently chiral molecule with intermolecular bonding capability.[17] In this work we demonstrate that the intermolecular interactions can be tuned by the presence or absence of coordinating metal atoms, i.e. adatoms which can be supplied by means of thermal deposition or by thermally activated release from the substrate. An irreversible conversion of 1D H-bonded assemblies of enantiomerically pure **1** to a Cu-coordinated chain assembly occurs. Surprisingly, in the H-bonded case, the opposite enantiomer leads to chains of inverted symmetry, whereas this is not the case for the metal-coordinated chains.

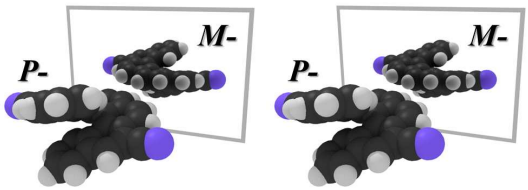

Figure 1 Enantiomers of 6,13-dicyano[7]helicene: (*P*)-**1** and its mirror image (*M*)-**1**.

All samples have been prepared and characterized in ultra-high vacuum (UHV). Molecules were deposited onto the substrates held at 90 K or 300 K, morphological assignment of the self-assembled structures was performed via STM at 5 K, unless mentioned otherwise, and the chemical environment of N-atoms in the CN-groups was characterized by XPS at room temperature (RT). Additionally, complementary DFT calculations have been used to model possible supramolecular arrangements (see SI for experimental and computational details).

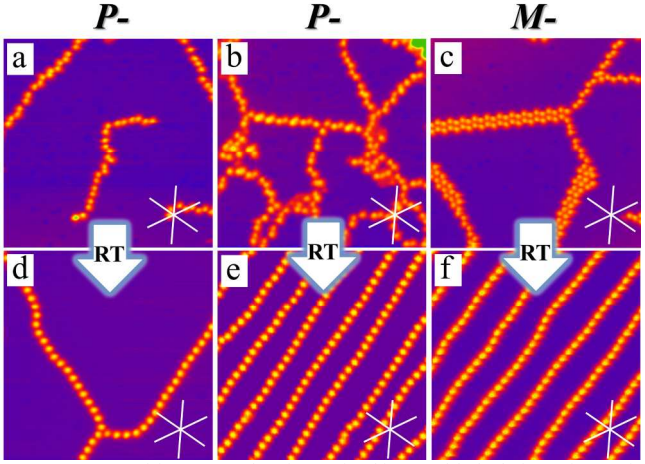

Figure 2. Transition, upon heating, of self-assembled chains of enantiopure **1** created by deposition at low (a) and higher (b, c) coverage of (a), (b) (*P*)-**1** or (c) (*M*)-**1** on cold (90 K) Cu(111) substrates (top row). Here coverages are significantly smaller than in our previous work.[17] Evolution of the chain morphology after heating to RT (bottom row). The STM images of enantiopure dicyano[7]helicenes taken at 5 K (30 x 30 nm^2; 25 pA; 1.2 V) reflect linear zig-zag shaped H-bonded self-assemblies and the subsequent formation of elongated islands at increased coverage created by a deposition of (a),(b) (*P*)-**1**-and (c) (*M*)-**1** onto a Cu(111) substrate held at 90K. (d-f) Formation of highly ordered molecular chains after annealing for 1 h at 300 K of the samples shown in (a), (b), and (c) respectively. Chains of both chirality senses, (*P*)-**1**-and (*M*)-**1**, are oriented 30° off the Cu(111) high-symmetry directions (indicated by white stars in each STM image).

STM experiments performed after deposition of enantiopure (*P*)-**1** or (*M*)-**1** on Cu(111) held at 90 K reveal assemblies, which are modified after heating to RT. STM data of enantiopure **1,** deposited on Cu(111) at 90 K, show a zig-zag chain organization for (*P*)-**1** (Figs. 2a,b) and for (*M*)-**1** (Fig. 2c). With increasing coverage, the well-separated zig-zag chains (Fig. 2a, ~0.05 mol/nm^2) evolve into irregular networks of chains, and linear supramolecular islands (Fig. 2b,c; ~0.17 mol/nm^2 and ; ~0.15 mol/nm^2 respectively). Interestingly, we observe also the directions of the chains to be independent of the chirality sense of the constituent molecules, namely along the directions rotated by 30° with respect to the principal axis of the Cu(111) surface. Heating of the samples to RT and re-investigation by STM at 5 K reveals a strongly modified morphology: Only long and straight chains occur which are oriented along the same crystallographic directions as before. The chain direction, again does not change with chirality sense ((*P*)-**1** (Fig. 2d,e) / (*M*)-**1** (Fig. 2f)). The evolution of zig-zag chains to linear chains has also been observed for the racemic mixture (±)-**1** (cf. S1). Importantly, at increased coverage, a new phase consists of large domains of parallel and quasi equidistant linear chains (cf. S2). We attribute this to repulsive electrostatic interactions (Fig. 2 e,f; chapt. 4 and 10 in SI), as was similarly assigned for Cu-pyridyl coordinated chains.[22] These complex phenomenological changes and the transition from chiral H-bonded zig-zag chains to straight linear chains with overall lack of chiral appearance (*vide infra*) hint at modified chain binding motifs after annealing, in agreement with CN-Cu assisted on-surface assembly.[23–25]

The chain architecture critically depends on the intermolecular interactions. The zig-zag structure of the chains formed at low (90K) sample temperature can be tentatively attributed to a balance between H-bonding (C–H···NC) and vdW interactions. In order to investigate the nature of the interactions in the straight chain assembly, we performed XPS study. For this purpose, we sublimed (*P*)-**1** onto Cu(111) and Au(111) surfaces kept at 300 K. The N1s binding energies of (*P*)-**1** correspond to 398.85 eV for submonolayer coverage on Au(111) and to 399.15 eV for a multilayer on Cu(111), respectively (cf. Fig. 3 and Fig. S4). These values correspond well with N1s XPS data for cyano substituents.[26] The significantly higher N1s binding energy for submonolayer coverage of (*P*)-**1** on Cu(111) (399.85 eV) evidences a different chemical environment of the nitrogen. Furthermore, only one N1s peak is observed, thus revealing equal bonding of both CN groups. Notably, the lone-pair of the N atom might interact with the Cu substrate. However, sp-hybridization of the cyano nitrogen and an energetically favorable σ-donor complexation to a metal (M) require a CN–M angle close to 180°. Therefore, this arrangement with both cyano groups simultaneously pointing to the surface is barely feasible (cf. Fig. 1). Note, that in the case of chemisorption of the CN groups and absence of their coordination, a N1s peak at lower binding energy (BE) would be expected.[27,28] Our observation of the N1s at higher BE provides an experimental evidence for the involvement of Cu adatoms in the intermolecular bonding and chain formation, which is additionally supported by the STM manipulations and DFT calculations (cf. S7 and chapt. 12 in SI).

In order to confirm the presence of Cu adatoms in the straight chain architecture, we evaporated a trace amount (~0.07 ML) of Cu onto the submonolayer of (*P*)-**1** on Au(111). In subsequently acquired XPS data, the N1s binding energy is shifted from 398.85 eV to 399.65 eV (Fig. 3a). STM measurements performed on the same sample at 77 K show straight chains (Fig. 3b). Conversely, in the absence of trace amounts of Cu, STM at 77 K reveals only a 2D condensed phase (cf. S5). These XPS and STM data confirm spontaneous coordination of (*P*)-**1** to Cu adatoms on Au(111). Notably, the Cu-coordinated chains are aligned along the herringbone reconstruction of the substrate (Fig. 3b). In particular, the pair of chains in closer proximity (~ 2nm) can be located at the linear hcp-domains, and the single chain follows the fcc-domains of the reconstruction (cf. Fig 3c, S6). Another interesting feature is the considerable variation in the intermolecular distance when the chains reorient by following the domains of the surface reconstruction. The range of variation (~1.2 ÷ 1.5 nm ± 0.1nm) is atypical for coordination complexes and may be attributed to the flexibility of the helicene backbone.

The observation of straight or zig-zag chains in dependence on the Cu(111) substrate temperature during deposition of

(*P*)-**1** or (*M*)-**1** is consistent with the above-described observations of the Cu coordination occurring after deposition of Cu adatoms on Au(111) held at room temperature. Notably, we observed the coexistence of linear and zig-zag chains after deposition of *(P)*-**1** on Cu(111) held at intermediate sample temperatures (~130 K). The availability of Cu adatoms from surface self-diffusion on Cu(111) depends primarily on the temperature among other factors (SI, chapt. 5). At the substrate temperature used to generate zig-zag chains (90K) the presence of Cu adatoms is significantly lowered[29], at further elevated temperatures CN-Cu complexes modify the chain (SI, chapt. 5).

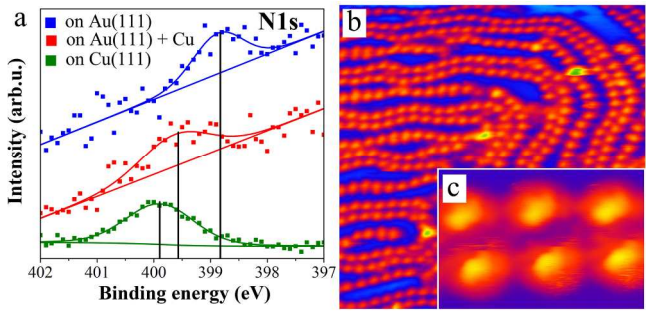

Figure 3 (a) XPS of submonolayer coverage of (*P*)-(–)-**1** on Cu(111) (green), Au(111) before (blue) and after (red) Cu addition. The presence of Cu adatoms significantly increases the N1s binding energy, thus confirming the formation of the Cu-coordination complex. (b) STM image (35 x 35 nm^2 ; 77 K) revealing Cu-coordinated (*P*)-**1** chains on Au(111), which are oriented along the linear domains of the herringbone reconstruction[30–32]. (c) High-resolution STM image (4.0 x 1.8 nm^2) of two neighboring chains on the hcp domain of the reconstructed Au(111) surface (cf. S6).

An important question with regard to the chirality of the building block relates to the degree of chirality transfer observable in the two different architectures, namely the H-bonded vs. the Cu-coordinated chains of (*P*)-**1** or (*M*)-**1**. The H-bonded chains of homochiral molecules appear as imperfect regular arrangement of dimers. However, far less defects occur in the chain after coordination to Cu. This is attributed to the thermodynamics of the system after being annealed, as well as to higher binding energy of the coordination bonds in comparison to H-bonds. Moreover, H-bonding can involve different aryl H atoms resulting in an aperiodic chain.[33] The most important difference between the two chain architectures lies in the presence or absence of mirror symmetry. For the H-bonded chains, the chirality of enantiopure (*P*)-**1** or (*M*)-**1** is reflected in the H-bonding pattern as mirroring of the dimers making the chain (Fig. 4a, c). In contrast, no such signature is observable after Cu coordination where the apparent repetitive unit consists of a single molecule only (Fig. 4 b, d).
DFT calculations have been performed to complement the experimental observations on (*M*)-**1** for the H-bonded (Fig. 4e) and Cu-coordinated chains (Fig. 4f). The simulated and experimental STM data were superimposed and show a good agreement. The calculations confirm the modification of the chain architecture (Fig. 4e and f, cf. S7-S9) with the transition of the bonding motif. As demonstrated in the side views in Fig. 4e and f, the dimers of the H-bonded chain derive from close contact interactions (H-bond, preferred to CN-Cu bonding and vdW) between two helicene molecules, leading to two non-equivalent positions of the CN groups involved in the bonding. ~~.~~ This non-equivalence implies that the chain exhibits a directional sense~~, defined by the bottom-to-top positions of the CN group in the molecular building blocks~~, and a~~. A~~ re-orientation of different segments within one chain is improbable due to the different ~~elevation of the H-bonds~~angle formed by the CN groups with respect to the substrate, as observed in Fig. 4e. After Cu-coordination, this non-equivalence is lifted by the flexure of the molecule to bind to the equidistant Cu adatoms. It seems that the strong coordination bond forces the helicene into the inter-adatom gap which is determined by the lattice registry. This occurs for both enantiomers and also for the racemate (cf. S1). The intermolecular distances, determined from the STM data, increase from 1.00 nm for the H-bonded chains to 1.35 nm for the Cu-coordinated chains. Experimental results and calculations of the proposed models are in good qualitative and quantitative agreement (SI, chapt. 9).

Concerning the chirality transfer in supramolecular on-surface arrays, the two types of helicene chains provide a very interesting model system: the same molecule forms two different chain arrangements by either weak H-bonding or relatively stronger coordination bonds. In this context, it is important to discuss the intermolecular and molecule-substrate interactions with respect to the orientation of the building blocks within the chain. Note, that all adsorbed helicenes of the same chirality sense can be aligned in the same manner by mere rotation and translation. Upon binding in a 1D chain, the CN-groups are fixed to the nearest neighbor molecules and exhibit a ~~lower~~ CN 'tail' and a ~~higher~~ CN 'head' with different angles with respect to the substrate. Thereby, different arrangements within one chain are possible. Due to the geometric constraints of the H-bonded architecture, tail-to-tail and head-to-head connections are more plausible than tail-to-head connections. This preference is confirmed in the simulated minimal energy arrangement (Fig. 4e, cf. S9). Further evidence is provided by the regularity of chains formed from enantiopure helicenes in comparison to the irregular arrangement of the racemic H-bonded chain on the same substrate.

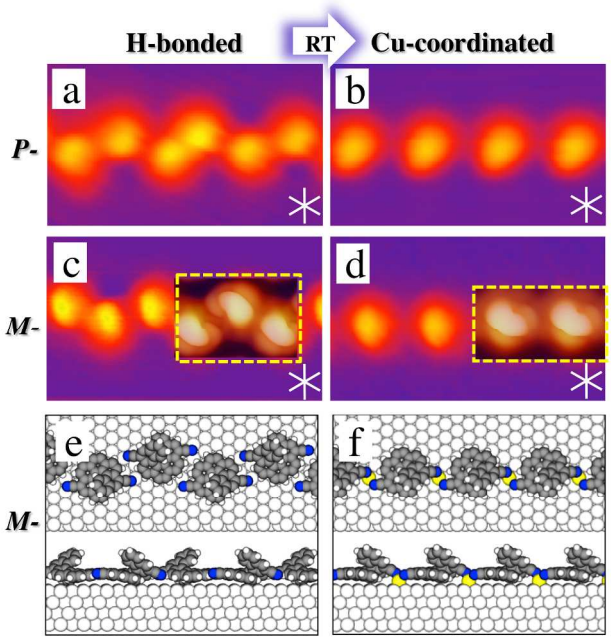

Figure 4. STM images (5.4 nm x 3.2 nm) of (*P*)-**1** and (*M*)-**1** on Cu(111) reveal a mirror-image appearance in H-bonded chains ((a) and (c), respectively). After coordination with Cu adatoms, the chains have a similar appearance ((b) and (d), respectively). The transition from one bonding motif to the other occurs by annealing for 1 h at 300 K. Simulated STM

images (marked by yellow dashed rectangles) of H-bonded (c) and Cu-coordinated (d) chains are superimposed onto the experimental ones. (e), (f) DFT models for H-bonded and metal-coordinated (*M*)-**1** chains.

Switching the point symmetry (chirality sense) of the building block from (*P*)-**1** to (*M*)-**1** leads to exact mirroring of the self-assembled chains: the characteristic 'dimers' recognized in the STM data are symmetry-inverted. The overall 'chain direction' with respect to the surface, however, remains the same. We attribute this observation to the high symmetry of the chain directions, i. e. <11$\bar{2}$> family of directions, which are mapped onto themselves upon symmetry inversion. After Cu coordination of the enantiopure (*P*)-**1** or (*M*)-**1**, the characteristic image of the chain is modified and two different orientations of the building blocks in the chain arrangement can be observed. These orientations are observed in random distribution, thereby all possible combinations occur: head-head, head-tail, and tail-tail (Fig. S12). This behavior indicates that the coordination bond, unlike the H-bond, does not differentiate between head-to-tail, head-to-head and tail-to-tail connections and thus, we do not observe mirror-image patterns in enantiopure Cu-coordinated chains. The racemic helicene forms Cu-coordinated chains along the same <11$\bar{2}$> directions. Stereoselectivity, which is a key factor in the assembly of the H-bonded chain, becomes negligible by the strong influence of the metal-coordination bond. This is confirmed in the numerical calculations by the limited flexure in H-bonded chains leading to non-equivalent bonding and by the considerable flexure of the helicenes after the stronger coordination bond is formed. This stronger binding in the chain i) flexes helicenes, ii) directs the chain formation in spite of small energy differences stemming from the different binding motifs (i.e. (3^2) for a racemate) and iii) overcomes non-equivalences in the molecular footprint of helicene on the corrugated substrate between the adatoms.

In general, molecular superstructures comprised of chiral elements on any surface give rise to mirror-inverted structures when the element of opposite chirality sense is used.[2] Our work demonstrates a remarkable exception, as the direction of helicene chains is independent of the chirality sense (*P* or *M*) of the molecular building block – neither in the case of the H-bonded nor in that of the Cu-coordinated chain. However, locally we observe that the symmetry of the H-bonded dimers is mirrored when the helicene of opposite chirality sense is used. By Cu coordination, the tolerance to symmetry and registry defects is observed to be increased considerably. Thereby, no spontaneous resolution is expected for 1D arrangements formed by Cu coordination. In conclusion, the complexity of intermolecular interactions – in the present case flexibility and weaker H-bonding vs. stronger Cu coordination - significantly affects the possibility of chiral recognition and spontaneous resolution.

ASSOCIATED CONTENT

Supporting Information

This information is available free of charge via the internet at http://pubs.acs.org.

AUTHOR INFORMATION

Corresponding Author

*Tel: +41 56 310 4518; E-mail: thomas.jung@psi.ch

Notes

The authors declare no competing financial interests.

ACKNOWLEDGMENT

We gratefully acknowledge the Financial support from the National Centre of Competence in Research Nanosciences (NCCR-Nano), Swiss Nanoscience Institute (SNI), Swiss National Science Foundation (grants No. 200020-137917, 206021-113149, 206021-121461), Wolfermann Nägeli Foundation and the Swiss Supercomputing Center (CSCS) for computational support. The authors sincerely thank S. Boz for her contribution during an early stage of this project, N. Ballav for the fruitful discussions, R. Pawlak, S. Kawai, R. Schelldorfer and M. Martina for support during measurements, and H. Rossmann for contribution to the graphics. The STM data were processed with the WSXM software.[34]

REFERENCES

(1) Shen, Y.; Chen, C.-F. *Chem. Rev.* **2012**, *112*, 1463–1535.
(2) Ernst, K.-H. *Phys. Status Solidi B* **2012**, *249*, 2057–2088.
(3) Gingras, M. *Chem. Soc. Rev.* **2013**, *42*, 1051.
(4) Flack, H. D. *Acta Crystallogr. A* **2009**, *65*, 371–389.
(5) Santagata, N. M.; Lakhani, A. M.; Davis, B. F.; Luo, P.; Buongiorno Nardelli, M.; Pearl, T. P. *J. Phys. Chem. C* **2010**, *114*, 8917–8925.
(6) Ortega Lorenzo, M.; Baddeley, C. J.; Muryn, C.; Raval, R. *Nature* **2000**, *404*, 376–379.
(7) Barlow, S. M.; Louafi, S.; Le Roux, D.; Williams, J.; Muryn, C.; Haq, S.; Raval, R. *Langmuir* **2004**, *20*, 7171–7176.
(8) Parschau, M.; Romer, S.; Ernst, K.-H. *J. Am. Chem. Soc.* **2004**, *126*, 15398–15399.
(9) Parschau, M.; Kampen, T.; Ernst, K.-H. *Chem. Phys. Lett.* **2005**, *407*, 433–437.
(10) De Cat, I.; Guo, Z.; George, S. J.; Meijer, E. W.; Schenning, A. P. H. J.; De Feyter, S. *J. Am. Chem. Soc.* **2012**, *134*, 3171–3177.
(11) Mugarza, A.; Lorente, N.; Ordejón, P.; Krull, C.; Stepanow, S.; Bocquet, M.-L.; Fraxedas, J.; Ceballos, G.; Gambardella, P. *Phys. Rev. Lett.* **2010**, *105*.
(12) Balandina, T.; W. van der Meijden, M.; Ivasenko, O.; Cornil, D.; Cornil, J.; Lazzaroni, R.; Kellogg, R. M.; De Feyter, S. *Chem. Commun.* **2013**, *49*, 2207.
(13) Fasel, R.; Parschau, M.; Ernst, K.-H. *Angew. Chem. Int. Ed.* **2003**, *42*, 5178–5181.
(14) Fasel, R.; Parschau, M.; Ernst, K.-H. *Nature* **2006**, *439*, 449–452.
(15) Taniguchi, M.; Nakagawa, H.; Yamagishi, A.; Yamada, K. *J. Mol. Catal. A Chem.* **2003**, *199*, 65–71.
(16) Parschau, M.; Fasel, R.; Ernst, K.-H. *Cryst. Growth Des.* **2008**, *8*, 1890–1896.
(17) Stöhr, M.; Boz, S.; Schär, M.; Nguyen, M.-T.; Pignedoli, C. A.; Passerone, D.; Schweizer, W. B.; Thilgen, C.; Jung, T. A.; Diederich, F. *Angew. Chem. Int. Ed.* **2011**, *50*, 9982–9986.
(18) Seibel, J.; Allemann, O.; Siegel, J. S.; Ernst, K.-H. *J. Am. Chem. Soc.* **2013**, *135*, 7434–7437.
(19) Hauke, C. M.; Rahe, P.; Nimmrich, M.; Schütte, J.; Kittelmann, M.; Stará, I. G.; Starý, I.; Rybáček, J.; Kühnle, A. *J. Phys. Chem. C* **2012**, *116*, 4637–4641.
(20) Rahe, P.; Nimmrich, M.; Greuling, A.; Schu□tte, J.; Stará, I. G.; Rybác□ek, J.; Huerta-Angeles, G.; Starý, I.; Rohlfing, M.; Ku□hnle, A. *J. Phys. Chem. C* **2010**, *114*, 1547–1552.
(21) Rybáček, J.; Huerta-Angeles, G.; Kollárovič, A.; Stará, I. G.; Starý, I.; Rahe, P.; Nimmrich, M.; Kühnle, A. *Eur. J. Org. Chem.* **2011**, *2011*, 853–860.
(22) Heim, D.; Écija, D.; Seufert, K.; Auwa□rter, W.; Aurisicchio, C.; Fabbro, C.; Bonifazi, D.; Barth, J. V. *J. Am. Chem. Soc.* **2010**, *132*, 6783–6790.
(23) Pawin, G.; Wong, K. L.; Kim, D.; Sun, D.; Bartels, L.; Hong, S.; Rahman, T. S.; Carp, R.; Marsella, M. *Angew. Chem. Int. Ed.* **2008**, *47*, 8442–8445.
(24) Sirtl, T.; Schlögl, S.; Rastgoo-Lahrood, A.; Jelic, J.; Neogi, S.; Schmittel, M.; Heckl, W. M.; Reuter, K.; Lackinger, M. *J. Am. Chem. Soc.* **2013**, *135*, 691–695.
(25) Pivetta, M.; Pacchioni, G. E.; Schlickum, U.; Barth, J. V.; Brune, H. *Phys. Rev. Lett.* **2013**, *110*.
(26) Lindberg, B.J.; Hedman, J. *Chem. Scripta* **1975**, *7*, 155–166.

(27) Sexton, B. A.; Hughes, A. E. *Surf. Sci.* **1984**, *140*, 227–248.
(28) Piantek, M.; Miguel, J.; Kru□ger, A.; Navío, C.; Bernien, M.; Ball, D. K.; Hermann, K.; Kuch, W. *J. Phys. Chem. C* **2009**, *113*, 20307–20315.
(29) Wang, W.; Shi, X.; Wang, S.; Van Hove, M. A.; Lin, N. *J. Am. Chem. Soc.* **2011**, *133*, 13264–13267.
(30) Fernandez-Torrente, I.; Monturet, S.; Franke, K.; Fraxedas, J.; Lorente, N.; Pascual, J. *Phys. Rev. Lett.* **2007**, *99*.
(31) Böhringer, M.; Morgenstern, K.; Schneider, W.-D.; Wühn, M.; Wöll, C.; Berndt, R. *Surf. Sci.* **2000**, *444*, 199–210.
(32) Yu, M.; Kalashnyk, N.; Barattin, R.; Benjalal, Y.; Hliwa, M.; Bouju, X.; Gourdon, A.; Joachim, C.; Lægsgaard, E.; Besenbacher, F.; Linderoth, T. R. *Chem. Commun.* **2010**, *46*, 5545.
(33) Wintjes, N.; Hornung, J.; Lobo-Checa, J.; Voigt, T.; Samuely, T.; Thilgen, C.; Stöhr, M.; Diederich, F.; Jung, T. A. *Chem. Eur. J.* **2008**, *14*, 5794–5802.
(34) Horcas, I.; Fernández, R.; Gómez-Rodríguez, J. M.; Colchero, J.; Gómez-Herrero, J.; Baro, A. M. *Rev. Sci. Instrum.* **2007**, *78*, 013705.

Insert Table of Contents artwork here